

Erosion Resistance of Cellulose Curing Agent Reinforced Sandy Loess

Jian Yang¹, Dan Zhao¹, Zhao Jin², Tao Tang² and Rui Gao^{3,4,*}

¹Shangluo, Shangluo Highway Bureau, 726000, China

²Shangluo Highway Administration Bureau Asphalt Plant, Shangluo, 726000, China

³College of Architecture and Civil Engineering, Xi'an University of Science and Technology, Xi'an, 710054, China

⁴Road Engineering Research Center, Xi'an University of Science and Technology, Xi'an, 710054, China

Received 19 June 2023; Accepted 20 October 2023

Abstract

Sandy loess is a kind of loess with a loose structure and, high sand content, and has negative effects on the overall stability of soil. To improve the stability of sand-sandy loess, this study proposed a chemically solidified sand-sandy loess by mixing two kinds of cellulose curing agents. Through direct shear test and triaxial compression test of sand-tests on the sandy loess soil before and after curing, the shear strength of sand-loess before and after curing was analysed, and the effects of the curing form and the ratio of mixed curing agents on the physical and mechanical properties of sand-loess soil were discussed. Next, the erosion resistance simulation test on solidified sand loess soil was carried out by using an indoor model test, and the simulation results were compared with the test results. On this basis, the main factors affecting the performance of solidified sand loess were analysed. Results show that, the curing effect of mixed curing agents is obviously superior to that of a single curing agent, and the shear strength of sandy loess increases with the concentration of the curing agent. With the increase of the curing soil's liquid-solid ratio of curing soil, the erosion quantity decreases gradually and reaches the minimum when the liquid-solid ratio is 1:2 and the slope is 30°, showing the best erosion resistance. The obtained conclusions provide some references to in determining the slope curing mode of sandy loess in practical engineering.

Keywords: Civil engineering, Sandy loess, Sodium carboxymethylcellulose, Polyacrylamide, Shear strength, Erosion resistance

1. Introduction

Sandy loess, a kind of loess with high sand content is a typical sediment in the desert-loess transition zone. This geological feature is primarily concentrated in a few provinces in Northern China, such as Shaanxi and Gansu, constituting a special geological environment. Sandy loess has poor geotechnical engineering properties, such as loose structure, low cohesive force, poor water stability and weak erosion resistibility. Compared with clayey loess or silty loess, the external environment can disturb sandy loess with extreme ease due to its loose and porous structure, thus triggering landslides, collapse and other geological disasters. Therefore, to provide effective reinforcement of sandy loess, a reasonable and effective reinforcement method with convenient construction and low cost is proposed, which is significant in improving the stability of sandy loess and decreasing geological disasters in sandy loess.

Compared with ordinary loess, sandy loess is difficult to be reinforced due to its special particle composition, soil mass structure and engineering properties. At present, associate studies mainly focus on chemical curing agents and microorganism curing method [1-6]. These two curing methods have a good reinforcement effect and can remarkably increase the shear and compressive strengths of the cured soil mass. However, in the practical engineering applications, the use of chemical curing agents for construction is simple but entails high costs. The microorganism curing method is complicated and the curing effect is often influenced by environmental factors, such as

the combination of recycled polyester fiber and SiO₂ [7], the abundant use of recycled polyester fiber may cause environmental pollution and restrict its large-scale application to practical engineering. Although the microbial induced carbonate precipitation (MICP) [8] processing technique solves the problem of environmental pollution, it has a moderate curing effect and fails to improve strength of sandy loess. Moreover, the technique is influenced greatly by the environment. Although the combination of PVA fiber and the MICP [9-11] processing technique improves the curing effect, it is restricted by the environment and difficult to be applied to practical engineering on a large scale.

To delete the malpractice of existing curing methods, ameliorate the poor geotechnical engineering properties of sandy loess and improve the physical and mechanical properties of sandy loess, considering the constraining influence of environmental factors on existing curing methods, this study proposes the preparation of a new type of curing agent to reinforce sandy loess by mixing cellulose curing agents, sodium carboxymethylcellulose (CMC) and polyacrylamide (PAM), which are harmless to the environment. Moreover, the physical and mechanical properties of the curing-agent-reinforced sandy loess were studied and the curing effect was evaluated.

2. State of the art

Sandy loess is easily affected by the external environment because of its loose pore structure and has poor physical and mechanical properties. Many scholars have conducted numerous studies on the physical and mechanical properties

*E-mail address: 1176701374@qq.com

ISSN: 1791-2377 © 2023 School of Science, IHU. All rights reserved.

doi:10.25103/jestr.165.24

of sandy loess, such as its shear strength, compressive strength and erosion resistance, by using many curing methods and proposing some curing methods suitable for engineering practice. However, the curing methods that have been studied are mainly focused on the curing of sandy loess with traditional admixtures. For example, Mengna Gao et al. [12] used bentonite-lime to improve the physical and mechanical properties of loess. The results show that the improvement method can effectively improve the compressive strength. Wei Fan [13] used cement to improve the unconfined compressive strength of loess and the loess engineering index parameters to evaluate its improvement effect. In the above studies, traditional admixtures, such as cement and lime, were mainly used to improve the physical and mechanical properties of sandy loess. However, the pH value around the building changes with the increase of the admixture amount, affecting the growth of vegetation, the groundwater quality, and soil productivity resulting in the decrease of the soil mechanical properties. Especially in the area where sand loess is widely distributed, nearly all slope projects must solidify sandy loess, resulting in a high negative impact on the environment.

To decrease the negative influences of admixtures on the environment, Gaochao Lin et al. [14] investigated the feasibility of improving the mechanical properties of sandy loess by using lignin and Canakci et al. [15] tested swelling soil samples modified by lignin, rice hull powder and rice hull ash. The results show that lignin can improve the unconfined compressive strength of modified soil. Furthermore, the liquid limit of modified soil decreases with the increase of the lignin content, but the plastic limit increases with the lignin content. In other words, the plastic index is negatively related to the lignin content. In the above studies, lignin is applied to effectively decrease the negative influences of additives on the environment. However, lignin is insoluble in water and complicated to operate in practical engineering projects, making its large-scale application difficult.

In improving the operability of cured sandy loess in practical engineering applications, scholars all over the world are facing difficulties in studying macromolecular curing agents, which are difficult to dissolve in water. Some studies show that the use of microorganisms with different fiber contents can increase the strength characteristics of sand samples, that is, enhance the unconfined compressive and splitting tensile strengths and improve the shear strength [16-18]. Meanwhile, cellulose can effectively improve the mechanical properties of sandy loess, providing a theoretical basis for using a cellulose curing agent to solidify sandy loess. Some scholars mixed sodium CMC and PAM and tested the mixture's cementation performance. They pointed out that due to the high cementation characteristics of CMC and the high linkage of the macromolecular chains in PAM, the soil curing layer formed among sandy soil particles has a dense network structure, so it can strengthen the water stability and increase the water retention capacity of soil particles [19-20]. With respect to the high-molecular polymer reinforcement mechanism of sandy soil, scholars at home and abroad have mainly focused on the chemical reaction of the hydration ions of polymers and the colloidal polymerization and mechanical properties of hyperlinked molecules. Some of the research results show that the hydrophilic carboxyl group (-COO-), hydroxyl, and other groups in modified CMC can act on sandy soil particles through physical effects, like crosslinking, adsorption, and bridging with the Si-OH, Ca²⁺, and Mg²⁺ on the surfaces of

sandy soil particles, thus making adjacent loose sandy soil particles form a network structure through macromolecular chains. Consequently, a curing layer of certain thickness is formed on the surface of sandy soil particles [21-22]. Shiqi Yang et al. [23] improved soil by using ammonium cellulose methyl carboxylate and found that it could effectively improve the soil moisture of arable soil. A cellulose modifier can adsorb water ions and the adsorption capacity increases with the concentration. In the above tests, a cellulose curing agent was used to solidify the sandy loess soil, but most scholars either studied the curing effect or mechanism of a single curing agent or the curing effect of mixed curing agents on sandy loess. Few scholars have proposed the best mix ratio of curing agents to solidify sandy loess.

In this study, focused on the inadequacy of existing studies, we suggest preparing a new curing agent by mixing CMC and PAM to increase the shear strength of sandy loess. The curing effects of single and mixed curing agents were compared in terms of shear strength. The scheme with the best curing effect was selected for the triaxial shear and erosion resistance simulation tests. The influences of the cellulose curing agents on the shear deformation and water erosion resistance of sandy loess were determined. The rainwater erosion resistance of the reinforced sandy loess was tested. Finally, the optimal concentration ratio of the cellulose curing agents in sandy loess was determined, aiming to achieve the optimal curing effect.

The remainder of this study is organized as follows. Section 3 discusses the test and test methods. Section 4 presents the analysis of the shear strength index of sandy loess before and after curing and the triaxial compressive and laboratory erosion resistance test results. The optimal mixing ratio of the two cellulose curing agents is provided. Section 5 summarizes the study and presents the conclusions.

3. Methodology

3.1 Experiment

3.1.1 Experimental materials

Sodium CMC and anionic PAM with a molecular weight of 10 million were selected as the cellulose curing agents. CMC is a carboxymethylated derivative of cellulose and is easy to dissolve in water. This cellulose curing agent forms a transparent agglomerated colloid solution after it is added to water, easily form films and can provide a gelatinization effect. PAM is a kind of high-molecular polymer whose molecular weight ranges from millions to tens of millions. PAM can dissolve in water at any form and ratio, and the aqueous solution formed is a transparent flocculent colloid. Under appropriate concentrations, the aqueous solution is presented as a network structure. The links of inter-chain machinery and hydrogen bonds intertwine into network nodes, thus providing flocculation, cementation, water retention and reinforcement to soil particles.

Test soil was collected from Yan'an of China. The soil in the area belongs to the typical slope sandy loess in loess plateau regions. Fig. 1 shows the grading curve of sandy loess and Table. 1 lists the basic physical properties. These show that the natural moisture content and liquid limit of sandy loess are relatively high.

3.1.2 Preparation of samples

Gravel and other impurities in the collected natural sandy loess samples were removed. Then, the sandy loess samples were dried in an oven to constant weight at 105 °C, ground,

and then screened using a 2 mm sieve. Single solutions of CMC and PAM and CMC+PAM mixed solutions were prepared. The mixing ratios of the curing agents are listed in Table. 2 and expressed in mass fraction of the curing agent. The cured sandy loess samples were prepared at liquid–solid mass ratios of 1:3 and 1:2. After mixing the different curing solutions evenly with sandy loess, the mixtures were placed in a closed container static for 24 h and sealed for later use.

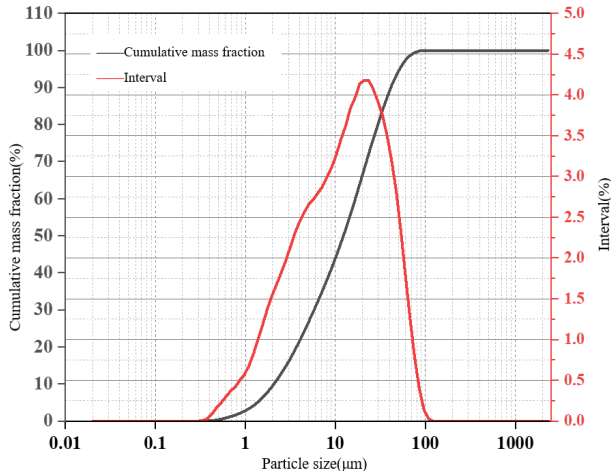


Fig. 1. Grading curve of sandy loess

strength and rigidity of materials through the loading-induced deformation of the samples. In this experiment, continuous loading was applied, and a constant vertical pressure was applied through a hydraulic jack. The apparatus was checked before the experiment to eliminate influences of the initial defect of the device and guarantee the normal operation of the devices and the instruments.



Fig. 2. Loading device in the experiment

3.1.3 Testing apparatus

The test loading device is shown in Fig. 2. The specimens were cylindrical, and the vertical loading mode was adopted. During field loading, the triaxial apparatus evaluates the

Table 1. Basic physical indexes of sandy loess

Soil sample	Natural water content (%)	Soil natural density (g·cm ⁻³)	Optimum water content (%)	Maximum dry density (g·cm ⁻³)	Liquid limit (%)	Plastic limit (%)
Sandy loess	17.15	1.34	17.54	1.4	32.8	22.2

Table 2. Mixing ratios of curing agents

Curing agents	Percentage concentration curing agents (%)					
	0.6	1.2	1.8	2.4	3	3.6
CMC	0.6	1.2	1.8	2.4	3	3.6
PAM	0.6	1.2	1.8	2.4	3	3.6
CMC+PAM	0.3+0.3	0.6+0.6	0.9+0.9	1.2+1.2	1.2+1.8	1.2+2.4

3.2 Test method

3.2.1 Direct shear test

Soil failure mainly refers to shear failure. The shear strength of soil mass can intuitively reflect its rainwater erosion resistance. Hence, the shear strength values of the reinforced sandy loess samples with different types of cellulose curing agents were evaluated through a direct shear test, revealing the optimal curing scheme and mixing ratio of curing agents. The liquid–solid ratio of the cured sandy loess samples in the direct shear test was 1:3, and the normal pressure was set to 100 kPa. After finishing the test, a shear strength envelope of soil was plotted by using normal pressure (σ) as the horizontal coordinate and shear stress (τ) as the vertical coordinate. The shear strength was calculated according to the Coulomb formula.

3.2.2 Triaxial compression test

Consolidated undrained triaxial compression test was performed on the cured sandy loess samples with different liquid–solid ratios and cement curing times. The variations of the principal stress difference and effective principal stress ratio of the cured sandy loess body were compared.

The cured sandy loess sample specification was 39.1 mm (diameter) × 80 mm (height), and the liquid–solid ratios were 1:2 and 1:3. The samples were prepared in four layers using the hierarchical pressing technique. After curing for 3 days, 7 days and 14 days under standard conditions, different confining pressures were applied in the test.

3.2.3 Laboratory simulation test of rainwater erosion resistance

The rainwater erosion resistance of the slope soil mass was evaluated in terms of the erosion resistance of the soil. Hence, the rainwater erosion status of the soil mass on the road slopes was simulated and the rainwater erosion resistance of the cured sandy loess samples was tested through a laboratory simulation test of the erosion resistance. The erosion resistance of soil is a property that characterizes the zero deformation of soil mass on water by resisting scouring with a structural binding force among soil particles. The soil structure with a strong erosion resistance is preferred and has a strong rainwater erosion resistance. Cured soil samples were prepared according to different liquid–solid ratios. The mixing ratio of curing agents was 1.2% CMC+2.4% PAM. All the samples were cured under

standard conditions for 3 days. Fig. 3 shows that the erosion resistance of the reinforced soil mass was tested with a slope erosion resistance simulation test device. The device is composed of a support, a steel water tank, a lifting chain, a soil moisture sensor, a water pump and a rainwater shower. The support size is 1.5 m (length) × 1.5 m (width) × 1.5 m (height). The water tank size is 1.8 m (length) × 1 m (width), and the plates at the two sides are 30 cm high. The soil moisture sensor can automatically record the slope soil moisture content during scouring every 1 min, and one scouring test takes 30 min, with a rainwater strength of 100 mm/h. The slope was controlled to 30°, 40° and 50°. Cumulative erosion quantity, which refers to the total soil particle mass eroded in one test, was used. On this basis, the erosion quantity of sand was calculated. All the sediment mass in the muddy water was weighed after draining rainwater. The dried weight of the sediments was taken as the erosion quantity of sand in the erosion test.

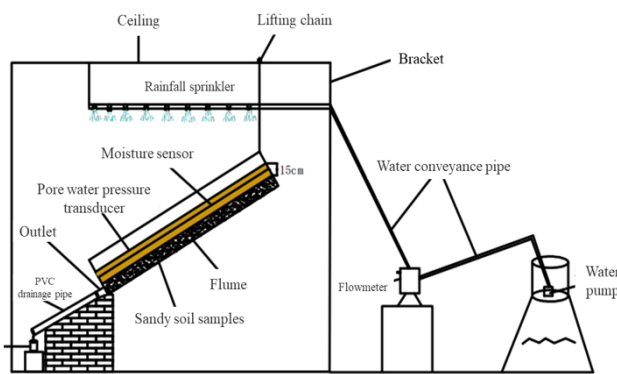


Fig. 3. Erosion resistance test device

4. Result Analysis and Discussion

4.1 Shear strength analysis of the cured sandy loess

The shear strength of the cured sandy loess was tested through a direct shear test. The curing effects of three types of curing agents were compared by analyzing the shear strengths under the same curing agent concentration. The relation curves between the curing agent concentration and shear strength of the cured sandy loess body under different curing schemes are shown in Fig. 4. After adding the cellulose curing agent in natural sandy loess, the shear strength remarkably increased. Given the same liquid–solid ratio, normal pressure and curing agent concentration, the shear strength of the sandy loess reinforced by the CMC+PAM mixture was higher than that of the sandy loess reinforced by a single curing agent. When the CMC concentration was 1.2%, the shear strength of the sandy loess reached the maximum. Subsequently, the shear strength declined gradually with the increase of the CMC concentration. When the CMC concentration reached 3%, the CMC powder was difficult to dissolve completely due to the excessive content. Hence, the shear strength of the cured sandy loess under high CMC concentrations was not tested in this study. With the addition of PAM and the CMC+PAM mixture, the shear strength of the sandy loess samples increased with the curing agent content. The maximum shear strength of the sandy loess samples was achieved when the PAM and CMC+PAM mixture concentrations reached 3.6%. Subsequently, the shear strength tended to stabilize, indicating that the curing effect reached saturation.

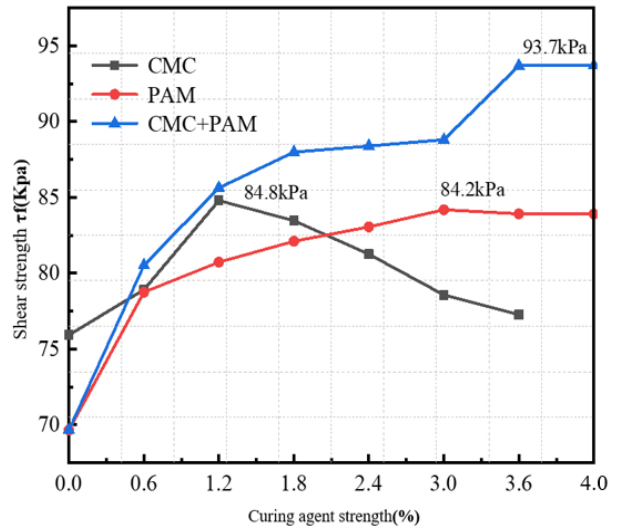


Fig. 4. Relation curves between concentrations of three types of curing agents and shear strength

The comparison of the direct shear test results indicates that under the same experimental conditions, the shear strength of the reinforced sandy loess with the CMC+PAM mixture is superior to that of the sandy loess reinforced by a single curing agent. This result reflects the superior curing effect of the CMC+PAM mixture over a single curing agent. Hence, the sandy loess reinforced by CMC+PAM mixture was selected in the follow-up tests.

The relation curves between the CMC+PAM mixture concentration and the shear strength of the reinforced sandy loess are shown in Fig. 5. Given the same liquid–solid ratio and curing agent concentration, the cohesive force and internal friction angle of the CMC+PAM cured soil increased with the curing agent concentration. Specifically, C increased from the initial 22 kPa to 38.22 kPa, increasing quickly when the curing agent concentration was 0%–1.2% but tended to stabilize after the curing agent concentration exceeded 1.2%. ϕ increased from the initial 25.5° to 27.61°, increasing when the curing agent concentration was 0%–1.2%, and exhibiting a sharp growth when the curing agent concentration exceeded 1.2%. In summary, the cohesive force and the internal friction angle increased with the CMC+PAM mixture concentration, indirectly proving that the CMC+PAM mixture concentration is positively related with the shear strength of the solidified soil. In other words, the higher the curing agent concentration is, the higher the shear strength of the solidified soil will be.

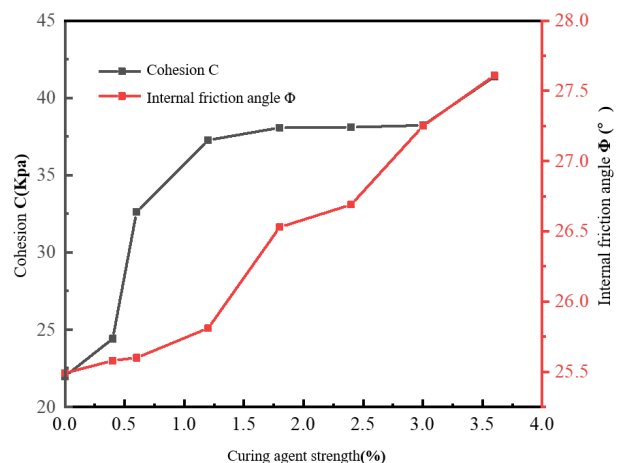


Fig. 5. Relation curves between CMC+PAM mixture concentration and shear strength

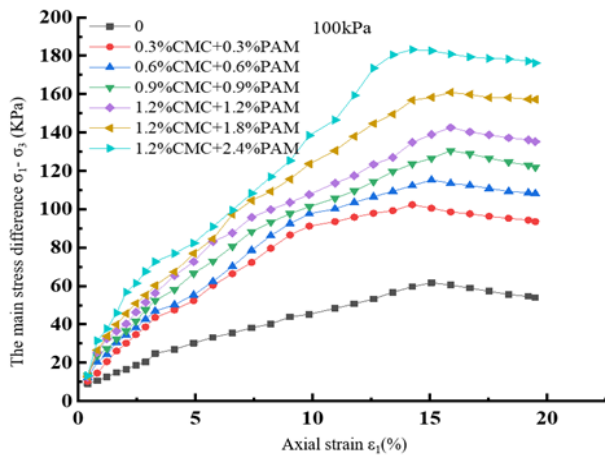
4.2 Analysis of triaxial compression test results

4.2.1 Relation between principle stress difference and strain

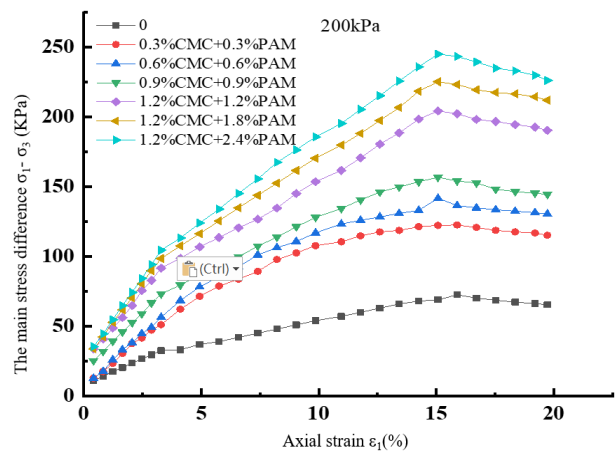
The stress–strain relations of the cured sandy loess with different CMC+PAM mixture concentrations at the liquid–solid ratio of 1:3 and the effective confined pressure of 100 kPa were analyzed through a consolidated undrained triaxial compression test. The samples were cured for 1 day. The principal stress difference was calculated according to Eq. (1):

$$\sigma_1 - \sigma_3 \square \frac{CR \times 10}{A_a} \tag{1}$$

where $\sigma_1 - \sigma_3$ is the difference between maximum principal stress and minimum principal stress. C is the calibration coefficient of the dynamometer, and R is the reading of the dynamometer. A_a is the correction section area of the samples.



(a) confining pressure = 100 kPa



(b) confining pressure = 200 kPa

Fig. 6. Stress-strain curves of reinforced sandy loess under different CMC+PAM mixture concentrations

4.2.2 Relationship between the principle stress ratio and strain

Fig. 7 shows that after adding CMC and PAM into the sandy loess, the effective principle stress ratio of the sandy loess increased with the axial strain. Given the same confining pressure, σ_1' / σ_3' is positively related with the curing agent concentration. According to the effective stress principle of saturated soil, the effective stress of soils determines the shear strength and deformation capacity of soil. The soil mass with the greater effective stress has the greater shear strength. As the CMC and PAM contents increased, the effective stress of the reinforced soil increased, thus increasing the shear strength of reinforced soil and improving the stability. Accordingly, the erosion resistance of the cured sandy loess was enhanced to the peak and then tended to stabilize.

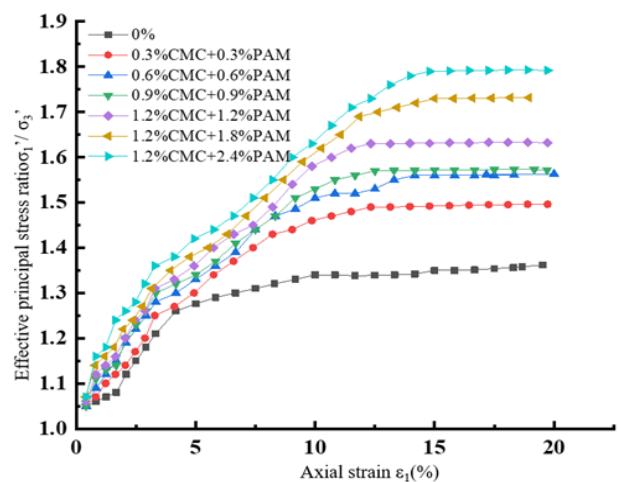


Fig. 7. Effective stress ratio and strain curve of reinforced soils under different curing agent concentrations

4.2.3 Compression deformation characteristics of reinforced sandy loess samples

Dilatancy deformation takes the dominant role during the triaxial compression of reinforced sandy loess samples. Soil mainly suffers from shear failure at compression. Fig. 8

generally shows the characteristics of coarse in the middle and slim at two ends because with the increase of the axial compressive deformation volume, the soil particles in the middle of the reinforced sandy loess samples are squeezed and develop lateral deformation. Soil particles slide and produce lateral friction. Adjacent particles move for separated occlusion and thereby produce occlusion friction. As the occlusion fails, the soil mass in the middle swells slowly, developing a dilatancy phenomenon. The sample height declines because of compression. Under undrained conditions, the stress and strain of the sandy loess at shearing behaviors show plastic flow. Soil particles rearrange under the action of shearing strength, thus causing changes in plastic volume and triggering plastic deformation.

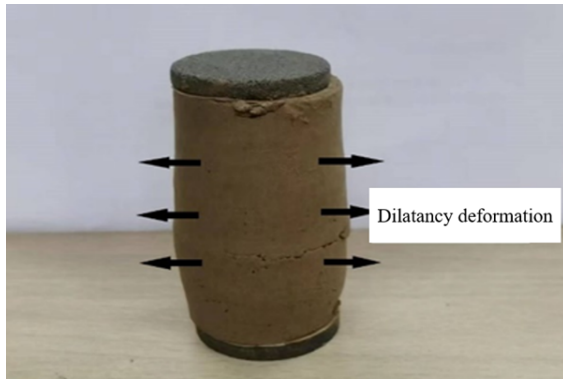


Fig. 8. Deformation characteristics of reinforced sandy loess samples

4.2.4 Relations of liquid-solid ratio and curing time with shear strength

The prepared sandy loess samples were cured for different times to make them bind fully. Subsequently, the shear strength of the cured sandy loess samples under different curing times and liquid–solid ratios was tested.

The shear strength of the cured sandy loess samples at different curing ages and under different liquid–solid ratios is shown in Table 3. The cohesive force and internal friction angle of the cured sandy loess in the test basically present a

consistent variation trend. They both increased with the liquid–solid ratio and curing time. According to the cohesive force results of the samples with different curing times, the shear strength of sandy loess with a liquid–solid ratio of 1:2 increased from 105 kPa at 3 days to 182 kPa at 14 days. The cohesive force increased by 73.3% compared with that at 7 days and by 42.7% from 127.5 kPa to 182 kPa. Thus, the cohesive forces of the cured sandy loess at 3 days, 7 days and 14 days remarkably differed. This result reflects that prolonging the curing time can improve the cohesive force of sandy loess to some extent.

The stress–strain relations at 3 days and 7 days under the liquid–solid ratio of 1:2 are shown in Fig. 9(a) and 9(b), respectively. The samples developed obvious deformation as axial strain occurred. Initially, the deviatoric stress increased quickly and then decreased slowly after reaching the peak, gradually stabilizing. Moreover, the stress difference at the failure of the reinforced soil samples increased with the effective confining pressure. The stress path curve of the reinforced sandy loess samples under 100 kPa, 200 kPa and 300 kPa increased along the same stress path in the beginning. The stress–strain curve presents a slow growth with the increase of strain, showing the shear hardening state. The formation of the stress–strain curve was simultaneously influenced by the confining pressure and the curing age. When the axial stress was within 0%–15%, the stress–strain curve presented strain hardening characteristics. After the strain exceeded 15%, the partial stress–strain curve exhibited strain softening characteristics after experiencing the peak stage. The principal stress difference (deviatoric stress) peak of the reinforced soil samples is relatively obvious, which occurred at the stress corresponding to the 10%–15% of the strain. Moreover, the peak strength increased with the curing times of the samples. The stress peak at 3 days was 445 kPa and increased by 237 kPa to 682 kPa at 7 days. The stress peak increased by 50% compared with that at 3 days, showing that the binding degree of the samples increased with the curing age, and the stress peak at failure increased accordingly, thus improving the stability of the cured soil.

Table 3. Shear strength of sandy loess samples under different liquid-solid ratio and curing time

Curing time		3 days		7 days		14 days	
		C(kPa)	$\phi(^{\circ})$	C(kPa)	$\phi(^{\circ})$	C(kPa)	$\phi(^{\circ})$
Liquid-solid ratio	1:2	105	14	127.5	18	182	20
	1:3	84.5	13	107	16	170.4	18

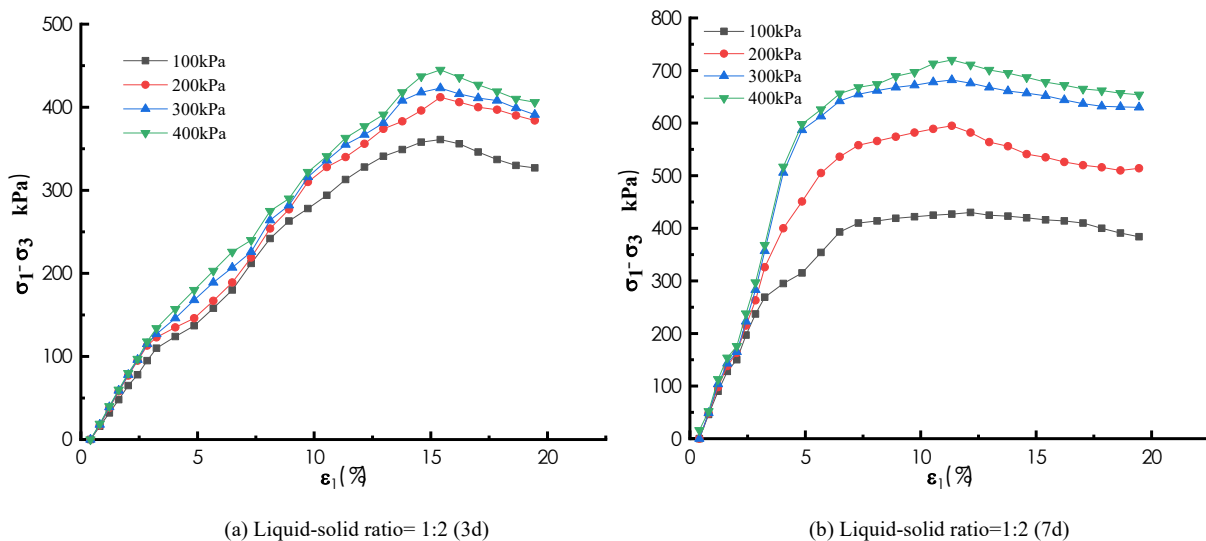


Fig. 9. Stress-strain relations of the cured sandy loess under different curing time

4.3 Laboratory simulation test results of erosion resistance

The erosion quantity of the cured soil slope under different liquid–solid ratios and slopes was compared through a laboratory simulation test of the rainwater erosion resistance. The influences of the liquid–solid ratio and slope on the erosion resistance of the slope were analyzed. The relationship between the slope of the cured soil and the erosion quantity under fixed liquid–solid ratio (1:3), rainfall intensity (100 mm/h), and curing time (3 days) is shown in Fig. 10. In the beginning of rainwater erosion, given that the water absorption rate of unreinforced soil is greater than its collapse rate, the unreinforced soil samples were not scoured by water in the first 5 min. After 5 min, the water absorption rate of the samples reached saturation, and the unreinforced soil samples softened after immersion in water. Given the extremely low binding strength and weak binding force of sandy soil particles, the internal structure of the samples was destroyed by immersion in water. The unreinforced soil began to collapse, scatter as particles and flow away with water. The reinforced soil slope was basically unscoured in the first 10 min because its water retention capacity was enhanced by the curing agent. Soil particles are connected into a network structure due to the adsorption effect among molecules, which enhances the internal structural stability of samples. Additionally, the erosion quantity of slope soil increases with the slope.

The erosion quantity of the cured soil slope was far lower than that of the unreinforced soil slope. The erosion quantity of the reinforced slope at 30°, 40° and 50° respectively decreased by 87.8%, 87.2% and 84.8% compared with those of the unreinforced slope. To sum up, the slope soil reinforced by curing agents can effectively decrease rainwater erosion and remarkably improve erosion resistance. The buried depth of the water moisture sensor was converted into the distance perpendicular to the slope surface and then divided by the time of arrival of water flow. In the approach, the average rainwater infiltration speed in this period could be calculated according to Eq. (2).

$$v \square \frac{h \cos \alpha}{t} \tag{2}$$

where v is the rainwater infiltration speed, h is the buried depth of the water moisture sensor, α is the slope, and t is the start of sensor operation.

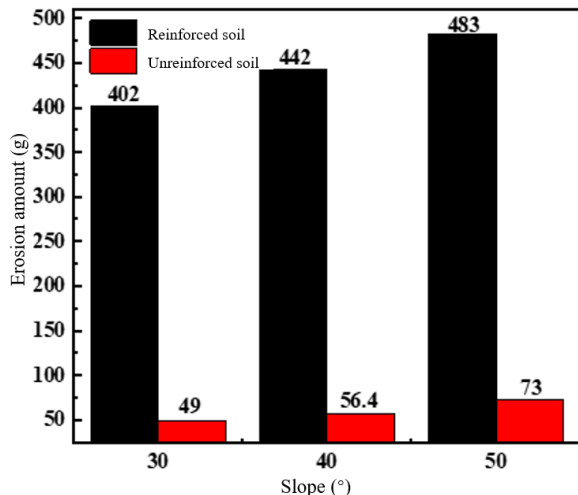


Fig. 10. Relation between slope and erosion quantity of samples

The relations of the liquid–solid ratio and erosion quantity of the sandy loess slope with the rainwater infiltration rate are shown in Fig. 11. Under the slope of 30° and 30 min of scouring, the erosion quantity of the unreinforced soil slope reached 437 g when the curing agent concentration was 0. At the liquid–solid ratio of 1:4, 1:3 and 1:2, the erosion quantity of the reinforced sandy loess was 85.2%, 88.8% and 93.6% lower than those of the unreinforced sandy loess, and the rainwater infiltration speed decreased by 41.6%, 57.5% and 61.7%, respectively. The erosion quantity declined considerably after adding the curing agent. With the increase of the liquid–solid ratio, the erosion quantity and the rainwater infiltration speed decreased gradually. This phenomenon indicates that the erosion quantity and rainwater infiltration speed of the slope soil can be decreased effectively by increasing the curing agent concentration.

The comparison of the sediment erosion form of reinforced and unreinforced soil slopes is shown in Fig. 12. Clearly, the soil structure of the reinforced soil slope was relatively complete after water erosion, without suffering obvious erosion failure. Nearly no soil particles were washed away, and the water flow was relatively clear, hardly containing any mud. On the contrary, the unreinforced soil slope displayed obvious erosion grooves from rainwater, accompanied with loose soil surface structures and many gullies. The erosion failure was worse than that in the reinforced soil slope. The washed soil content was high, and the water flow was muddy, containing many sandy soil particles. The overall stability was poor compared with that of the reinforced soil slope. Hence, reinforced soil slope can effectively resist rainwater erosion.

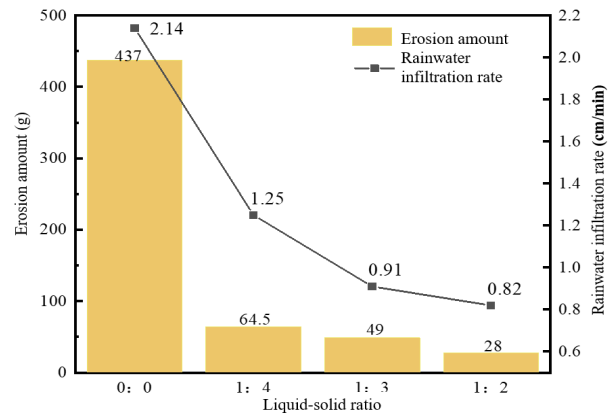


Fig. 11. Relations of liquid-solid ratio and erosion quantity and rainwater infiltration speed



Fig. 12. Comparison of erosion forms of reinforced and unreinforced soil slopes

5. Conclusion

To enhance the water stability and erosion resistance of sandy loess slope and improve the water and soil loss phenomenon, the study prepared a new cellulose curing agent reinforced sandy loess slope by mixing CMC and PAM. Through the direct shear, triaxial compression, and laboratory simulation test of erosion resistance, the shear strength, compressive deformation characteristics, erosion resistance, and other relevant indexes of the reinforced sandy loess were analyzed. The following major conclusions could be drawn.

(1) The curing effect of sandy loess is improved by extending the curing time and increasing the liquid–solid ratio of the curing agent. The cohesive force at 14 days shows an increase of 43.36% compared with that at 7 days and 73.64% compared to that at 3 days. The stress peak at 7 days exhibits an increase of approximately 50% of that at 3 days. At the same curing age, the cohesive force of the cured sandy loess with a liquid–solid ratio of 1:2 increased significantly compared with that at 1:3.

(2) The erosion resistance of the curing agent reinforced sandy loess is significantly higher than that of the unreinforced samples. The erosion resistance of the cured soil increases with the liquid–solid ratio. The erosion quantity of sandy loess increases with the slope but decreases with the increase of the liquid–solid ratio. The minimum erosion quantity of the reinforced soil slope is achieved when the liquid–solid ratio is 1:2 and the slope is 30°.

The proposed CMC+PAM mixture reinforcement effectively increases the shear strength and erosion resistance of the sandy loess. This approach provides a new idea for the reinforcement of sandy loess slope. However, few test groups for different concentrations of CMC and PAM were used, and limited relevant indexes were obtained. The optimal mixing ratio of CMC and PAM requires further investigation.

This is an Open Access article distributed under the terms of the Creative Commons Attribution License.



References

- [1] M. E. Kortbawi, D. M. Moug, K. Ziotopoulou, J. T. DeJong, and R. W. Boulanger, "Axisymmetric simulations of cone penetration in Biocemented sands," *J. Geotech. Geoenviron. Eng.*, vol. 148, no. 11, Nov. 2022, doi: 10.1061/(ASCE)GT.1943-5606.0002914.
- [2] V. N. Pham, E. Oh, and D. E. Ong, "Effects of binder types and other significant variables on the unconfined compressive strength of chemical-stabilized clayey soil using gene-expression programming," *Neural. Comput. Appl.*, vol. 34, no. 11, pp. 9103-9121, Jun. 2022, doi:10.1007/s00521-022-06931-0.
- [3] Z. Faeli, B. M. Montoya, and M. A. Gabr, "Various Bacterial Attachment Functions and Modeling of Biomass Distribution in MICP Implementations," *J. Geotech. Geoenviron. Eng.*, vol. 149, no. 9, Sep. 2023, doi: 10.1061/JGGEFK.GTENG-10812.
- [4] N. Banik, R. Sarkar, and M. E. Uddin, "Assessment of strength and low-strain shear modulus of bio-cemented sand considering MICP treatment," *Environ. Earth Sci.*, vol. 82, no. 4, Feb. 2023, doi: 10.1007/s12665-023-10780-y.
- [5] N. Roy, J. Frost, and D. Terzis, "3-D contact and pore network analysis of MICP cemented sands," *Granular Matter*, vol. 25, no. 4, Nov. 2023, doi: 10.1007/s10035-023-01347-6.
- [6] M. Sarkis, M. Abbas, A. Naillon, F. Emeriault, C. Geindreau, and A. Esnault-Filet, "DEM modeling of biocemented sand: Influence of the cohesive contact surface area distribution and the percentage of cohesive contacts," *Comput. Geotech.*, vol. 149, Sep. 2022, doi: 10.1016/j.compgeo.2022.104860.
- [7] J. M. Sarli, F. Hadadi, and R. A. Bagheri, "Stabilizing geotechnical properties of loess soil by mixing recycled polyester fiber and nano-SiO₂," *Geotech. Geol. Eng.*, vol. 38, no. 8, pp. 1151-1163, Oct. 2020, doi: 10.1007/s10706-019-01078-7.
- [8] Z. Faeli, B. M. Montoya, and M. A. Gabr, "Elucidating factors governing MICP biogeochemical processes at macro-scale: A reactive transport model development," *Comput. Geotech.*, vol. 160, Aug. 2023, doi: 10.1016/j.compgeo.2023.105514.
- [9] X. C. Gao, S. K. Han, Y. Yang, W. Zhang, T. Zou, and L. Cheng, "Mechanical behavior and microstructural study of biocemented sand under various treatment methods," *Geofluids*, vol. 2022, Apr. 2022, doi: 10.1155/2022/6015335.
- [10] S. G. Choi, T. Hoang, E. J. Alleman, and J. Chu, "Splitting tensile strength of fiber-reinforced and biocemented sand," *J. Mater. Civ. Eng.*, vol. 31, no. 9, Sep. 2019, doi: 10.1061/(ASCE)MT.1943-5533.0002841.
- [11] G. Amarakoon, and S. Kawasaki, "Factors affecting sand solidification using MICP with *Pararhodobacter* sp.," *Mater. Trans.*, vol. 59, no. 1, pp. 72-81, Jan. 2018, doi: 10.2320/matertrans. M-M2017849.
- [12] M. N. Gao, X. Wang, J. D. Li, Y. J. Zhang, and D. J. Jiang, "Experiment study on the strength and microstructure of bentonite-lime improved loess," (in Chinese), *Hydro-Sci. Eng.*, vol. 2022, no. 5, pp. 86-94, Oct. 2022.
- [13] W. Fan, "Research on improving collapsible loess by cement," (in Chinese), *Value Eng.*, vol. 41, no. 18, pp. 64-66, Sep. 2022.
- [14] G. C. Lin, W. Liu, J. Zhao, and P. Fu, "Experimental investigation into effects of lignin on sandy loess," *Soils Found.*, vol. 63, no. 5, Oct. 2023, doi: 10.1016/j.sandf.2023.101359.
- [15] H. Canakci, A. Aziz, and F. Celik, "Soil stabilization of clay with lignin, rice husk powder and ash," *Geomech. Eng.*, vol. 8, no. 1, pp. 67-79, Jan. 2015, doi: 10.12989/gae.2015.8.1.067.
- [16] R. Cardoso, J. Vieira, and I. Borges, "On the use of biocementation to treat collapsible soils," *Eng. Geol.*, vol. 313, Feb. 2023, doi: 10.1016/j.enggeo.2022.106971.
- [17] A. Karami, I. Shooshpasha, and H. A. Alikhani, "Effects of *Sporosarcina Pasteurii*'s on Curing Time and Strength of Silty Sand Soil," *Geotech. Geol. Eng.*, vol.41, no.6, pp.3289-3304, Jun. 2023, doi: 10.1007/S10706-023-02454-0.
- [18] R. F. Rodríguez, and R. Cardoso, "Study of biocementation treatment to prevent erosion by concentrated water flow in a small-scale sand slope," *Transp. Geotech.*, vol. 37, Nov. 2022, doi: 10.1016/j.trgeo.2022.100873.
- [19] F. X. Kong, D. Yang, J. Liu, Y. Wang, X. Chen, X. Shi, and et al., "Experimental study on consolidation characteristics of sand improved by polyurethane curing agent," (in Chinese), *Invest Sci Technol*, no. 4, pp. 1-6, Aug. 2019.
- [20] J. H. Wu, W. H. Tao, H. Y. Wang, and Q. Wang, "Effects of Sodium Carboxymethyl Cellulose on Soil Aggregate Structure and Water Movement Characteristics," (in Chinese), *Trans. Chin. Soc. Agric. Eng.*, vol. 31, no. 2, pp. 117-123, Jan. 2015.
- [21] Y. T. Wang, K. Yang, and Z. J. Tang, "Effect of fly ash-and polyacrylamide-consolidated soil layer on *A. splendens* growth in a desert in North China," *Catena*, vol. 210, Mar. 2022, doi: 10.1016/j.catena.2021.105935.
- [22] H. Jume, S. R. Ning, Q. J. Wang, and J. Zhang, "Effects of PAM and CMC on soil water infiltration and evaporation characteristics," (in Chinese), *J. Soil Water Conserv.*, vol. 34, no. 1, pp. 121-127+134, Feb. 2020, doi: 10.13870/j.cnki.stbxb.2020.01.018.
- [23] S. Q. Yang, L. Xing, H. Y. Liu, W. S. Wang and P. Guo, "Effects of carboxymethyl cellulose ammonium on soil properties of newly cultivated land in Loess Plateau," (in Chinese), *J. Northwest A & F Univ. (Nat. Sci. Ed.)*, vol. 49, no. 5, pp. 74-80, May. 2021, doi: 10.13207/j.cnki.jnwafu.2021.05.010.